Superficial Wrinkles in Stretched, Drying Gelatin Films

R. Rizzieri,[‡,§] L. Mahadevan,[*,†] A. Vaziri,[†] and A. Donald[‡]

Division of Engineering and Applied Sciences, Harvard University, 29 Oxford Street, Pierce 324, Cambridge, Massachusetts 02138, and Polymers and Colloids Group, Physics Department, Cavendish Laboratory, University of Cambridge, Madingley Road, Cambridge CB3 0HE, U.K.

Received August 27, 2005. In Final Form: November 17, 2005

When a thin film of initially hydrated gelatin is allowed to dry from the surface, superficial changes in the structure of the material affect the local mechanical properties of the drying region. If the film is simultaneously subjected to large strain deformation (above 20%), a periodic pattern of wrinkles appears on the surface of the gelatin along the length of the sample in the direction of the applied force. These wrinkles are uniformly distributed on the surface of the gelatin with a wavelength that is much smaller than the sample thickness, which changes with sample composition, aging time, and deformation rate. We investigate these patterns via in situ environmental scanning electron microscopy (ESEM) and provide a theory for their origin.

1. Introduction

Understanding the role of water in determining the microstructural origins of the mechanical behavior of soft gels, colloids, and emulsions is a problem that is faced everyday in the food and personal care industry. This requires the ability to simultaneously monitor the microstructure and control the environmental humidity and hydration levels of the sample as it is loaded or unloaded. Recently, it has become possible to carry out a mechanical test inside an electron microscope that can still keep the sample in its natural state. The environmental scanning electron microscope (ESEM) like all scanning electron microscopes (SEMs), offers the possibility of imaging specimens at very high resolution (up to a few nanometers in favorable cases). In addition, the ESEM allows the study of hydrated materials as close to their natural state as possible, in such a way that structural evolution due to mechanical deformation can be visibly followed. This is achieved by controlling the pressure inside the specimen chamber; a pressure as high as 20 Torr (∼2.5 kPa) may be employed, using water vapor as the gas in the specimen chamber, with no coating required due to the ionization process occurring during the imaging process.[1] If the specimen temperature is held constant, an increase or decrease in the partial pressure of water vapor results in condensation or dehydration, respectively. This ability to control the environment allows us to study gels,[2] emulsions,[3] drying thin-film coatings,[4] foams, and food[5] in their natural states.

A detailed description of the experimental technique adopted is given elsewhere.[2,6] An example of such an experiment is the real-time observation of deformation and failure of materials under an applied load.[7] A straining rig can be used to place samples in different loading conditions. It is thus possible to relate the typical response of a material, obtained through mechanical data, to its microstructural behavior.[8]

Here we use the ESEM to study the large deformation behavior of a ubiquitous hydrated polymeric gel gelatin in a hydration-controlled environment. Our initial goal was to characterize the mechanical properties of gelatin in the small and large deformation regimes. However, during the course of the experiments, we found a periodic surface pattern that arises naturally; thus, the primary focus here is to characterize and explain these hierarchical wrinkling patterns.

2. Materials and Methods

Gelatin gel was obtained by alkaline degradation of collagen. A gelatin solution was prepared by dissolving the powder (18% w/w) at 60 °C for 30 min in deionized water (containing 0.1 M NaCl). Sodium azide (∼500 ppm) was added to prevent bacteriological degradation of the gelatin. When the solution is cooled below ∼28 °C, a three-dimensional gel network appears, with the gelatin chains linked by triple helices.[9] Ethylene glycol was also used in place of water as a solvent for gelatin solutions. The lower volatility of ethylene glycol compared with water makes it an interesting alternative solvent for solvated biopolymer specimens during dynamic tests. Samples made with photographic grade gelatin were also tested to demonstrate the generality of response of different gelatin gels, all of which behave in a similar way under comparable applied conditions. Salt (NaCl) was added to some samples.

The biopolymer solution was poured onto an aluminum frame fixed on an aluminum mold covered with Parafilm M to prevent sticking. An aluminum plate covered in Parafilm M was placed on the solution to seal the sample, and a weight of about 500 g was placed on the top to ensure a uniform thickness of the sample. The mold was then stored in the fridge at 7 °C for at least 24 h prior to testing.[2] Samples were cut from the thin gelled sheet using a "dog-bone" shaped cutter (10 mm gauge length and 4 mm width). The sample was then glued using a cyanoacrylate adhesive on one side of two aluminum specimen holders. As can be seen from Figure 1, the sample was glued onto flat aluminum strips punctured such that they could be dropped over pegs mounted on both jaws of the tensometer, one of which was attached to the load cell. The sample was laid down so that it was in contact with the cooled bar, until

* Corresponding author. Address: DEAS, Harvard University, 29 Oxford Street, Cambridge, MA 02138. E-mail: lm@deas.harvard.edu.

† Harvard University.

‡ University of Cambridge.

§ Present address: CMIC−Dipartimento di Chimica, Materiali e Ingegneria Chimica, Politecnico di Milano, Piazza Leonardo da Vinci, 32, 20133 Milano, Italy.

(1) Donald, A. M. *Nat. Mater.* **2003**, *2*, 51−56.
(2) Rizzieri, R.; Baker, F. S.; Donald, A. M. *Polymer* **2003**, *44*, 5927−5935.
(3) Stokes, D. J.; Thiel, B. L.; Donald, A. M. *Langmuir* **1998**, *14*, 4402−4408.
(4) Keddie, J. L.; Meredith, P.; Jones, R. A. L.; Donald, A. M. *Macromolecules* **1995**, *28*, 2673−2682.
(5) Donald, A. M. *Curr. Opin. Colloid Interface Sci.* **1998**, *3*, 143−148.
(6) Rizzieri, R.; Baker, F. S.; Donald, A. M. *Rev. Sci. Instrum.* **2003**, *74*, 4423−4428.
(7) Stokes, D. J.; Donald, A. M. *J. Mater. Sci.* **2000**, *35*, 599−607.
(8) Thiel, B. L.; Donald, A. M. *J. Texture Stud.* **2000**, *31*, 437−455.
(9) Bot, A.; van Amerongen, I. A.; Groot, R. D.; Hoekstra, N. L.; Agterof, W. G. M. *Polym. Gels Networks* **1996**, *4*, 189−227.

10.1021/la052343m CCC: $33.50
Published on Web 03/18/2006 PAGE EST: 4.9

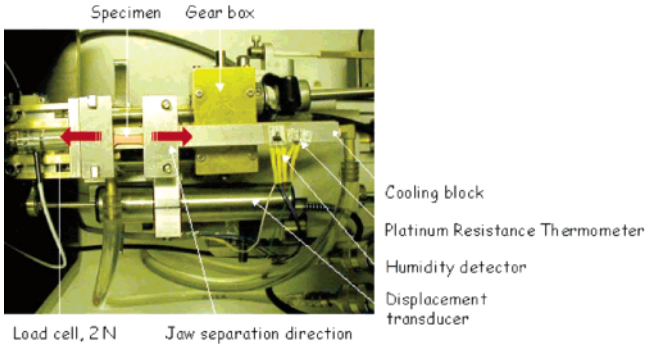

Figure 1. Photo of the tensometer with its components for testing samples within the specimen chamber of the ESEM. The arrows indicate the direction of the jaw separation. The gearbox is connected to a stepper motor attached to the door of the ESEM chamber. The "dog-bone" shaped gelatin sample is glued onto the aluminum specimen holders, designed to be dropped onto the tensometer. The shape of a dog-bone is obtained by pressing on the gelatin with a specially designed steel "cookie" cutter. The sample is in contact with the cooling block before starting the test. Once the strain is applied, the sample lifts itself up by about 1 mm from the cooling block. Only the initial part of the stress−strain curve (approximately for the first 0.1% strain) is corrupted by the sample stick-slipping on the cooling block. A more detailed explanation can be found in ref 6.

such time as the strain was applied. As the deformation proceeded, the sample lifted up slightly from the cooling block. It is assumed that this occurred because of slight thinning of the sample as it stretched. As stretching advanced, the sample distance from the cooling block (approximately 1 mm) was constant during the test. This small distance between the sample and the cooling stage removed any interference to the measurements due to stick-slip and water condensation on the sample, yet ensured good temperature control of the sample. Prior to running the experiment, the cooling block responsible for keeping the sample at a controlled temperature during the whole experiment was equilibrated at the test temperature of 2 °C. Tensile tests were performed at a strain rate of approximately 0.001 s^{-1} at controlled humidity and temperature.

Specimens were imaged using an ElecroScan 2010 ESEM equipped with a tungsten hairpin filament. The beam energy was 20 kV, and the signal was collected using a gaseous secondary electron detector (GSED). Geometric constraints of the mechanical stage limited the working distance to no less than 8.5 mm. Water vapor was used as the imaging gas, with constant pressure of ∼5 Torr. The temperature was maintained at 2 °C during pump-down and the duration of the whole experiment. The experimental conditions and an accurate description of the tensometer built for these experiments have been previously described.[2,6] This construction permitted load-extension curves to be determined for hydrated samples simultaneously with imaging while maintaining the sample in its fully hydrated state, thus providing a unique opportunity to explore the structure and dynamic mechanical characteristics of the moist system. During all the tests, the experimental conditions were kept identical to compare the results. Tensile stages have been fitted in the ESEM before,[7,8] but, in this case, the instrument has been modified to keep the sample moist during the entire application of the strain, as described in ref 6.

For materials that exhibit relatively large strain at failure (i.e., > 10%), such as gelatin gels, correction must be made for the reduction in cross-sectional area that occurs during deformation.[10] The corrected failure stress, named "true" stress, is defined as the load (F) divided by the instantaneous cross-sectional area (A):

$$\sigma_T = F/A \tag{1}$$

(10) Young, R. J.; Lovell, P. A. *Introduction to Polymers*; Chapman and Hall: London, 1991.

For the gelatin gels studied in the present work, the deformation during tensile testing can be approximated to occur at a constant volume, and so A can be related to the original cross-sectional area A_0 through the equation

$$AL = A_0L_0 \tag{2}$$

where L_0 and L are the original and instantaneous gauge lengths, respectively. The true stress is thus defined as

$$\sigma_T = FL/A_0L_0 \tag{3}$$

Similarly, the corrected strain, termed "true" strain, ϵ_T, is

$$\epsilon_T = \ln(L/L_0) \tag{4}$$

The elastic modulus in tension is then given by

$$E_T = \sigma_T/\epsilon_T \tag{5}$$

During this study, the parameters that identified the level of damage occurring during deformation are true stress and true strain; the instantaneous gauge lengths (L) are assumed to be the same as the distance between the clamps.

3. Results and Discussion

A series of ESEM images showing the typical evolution of the surface morphology of a gelatin gel sample recorded simultaneously while applying strain is shown in Figure 2. The arrows in Figure 2A show the direction of the applied strain for both the tensometer and the micrograph, and these directions are constant for all micrographs. A characteristic true stress/strain curve is also shown in Figure 2. Three different load regimes were observed to be representative of the gelatin biopolymer behavior under applied strain at constant strain rate. At low strains (<20%) no change in the surface morphology was observed. The micrograph looked identical to the ones taken of the unstrained sample. At larger strains (> 20%), rather unexpectedly, a series of regular bands aligned along the direction of the applied strain appeared, as shown in Figure 2B. The sample thickness (∼2 mm) is much greater than the wrinkle wavelength, and the banding is a surface feature that decays into the bulk, as can be seen in a view of the fractured edge of a sample (Figure 3). The wrinkles first appear at the top and bottom surfaces, but subsequently are also seen all the way around the sample. Further loading causes surface cracks to open (Figure 4E), exposing fresh gelatin, which is initially smooth and flat. However as straining continues, bands are also seen to appear on these inner crack surfaces (Figure 4F) but with a different periodicity from those on the top/bottom surfaces of the samples. Finally, failure occurs at strains of ∼85%. As the sample breaks, the stress is relaxed, and the pattern of banding changes dramatically. Very beautiful and complex patterns form as the stress is relieved (Figure 5). The initial bands are now crossed transversely by a second periodic pattern, so that a zigzag appearance results. After breakage, the samples curl in the direction of the bands. If the broken sample is immersed in water, it curls in the opposite direction, again suggesting that the surface water content may be crucial in determining the behavior of the sample. However, the precise pattern found upon breakage depends on how long the sample has been under strain. Figure 5A shows the surface pattern of a sample held under stress longer than the sample shown in Figure 5B. We will not attempt to explain these failure patterns in detail, but merely note that the time under stress, corresponding to the time during which surface dehydration may occur, has a significant effect on the failure pattern.

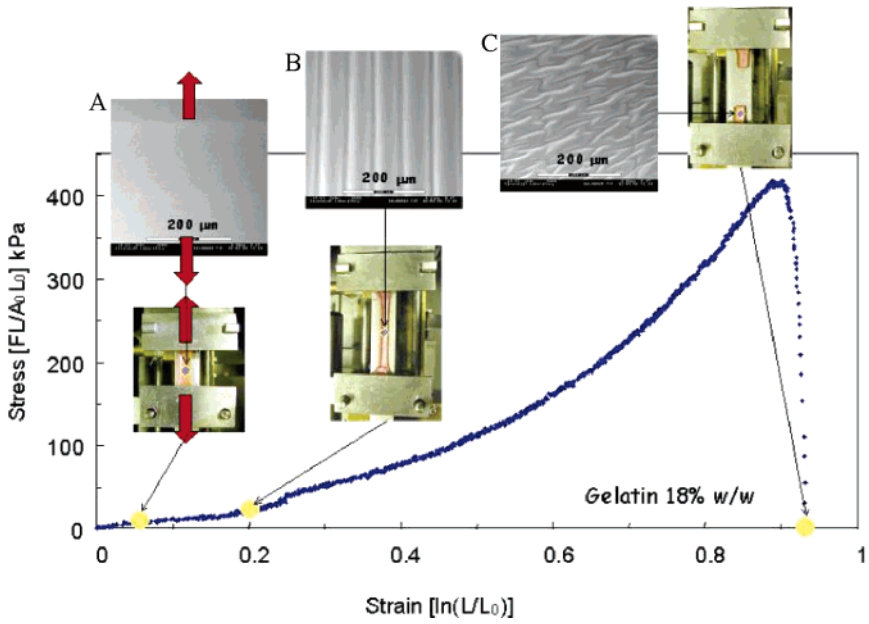

Figure 2. In situ stress−strain plot for a "typical" tensile test on a gelatin sample in the ESEM. Three characteristic points on the tensile tests are illustrated at the top of the diagram, each with an ESEM micrograph of the mixture surface during stretching. The direction of the applied strain is vertical. (A) At low strain, the sample surface is identical to the unstrained sample surface. (B) At about 20% strain, the sample surface shows the presence of regular bands on the surface of the biopolymer. The direction of the applied strain is the same as the direction of the bands. (C) When the sample breaks, the folds on the surface relax, forming a regular pattern.

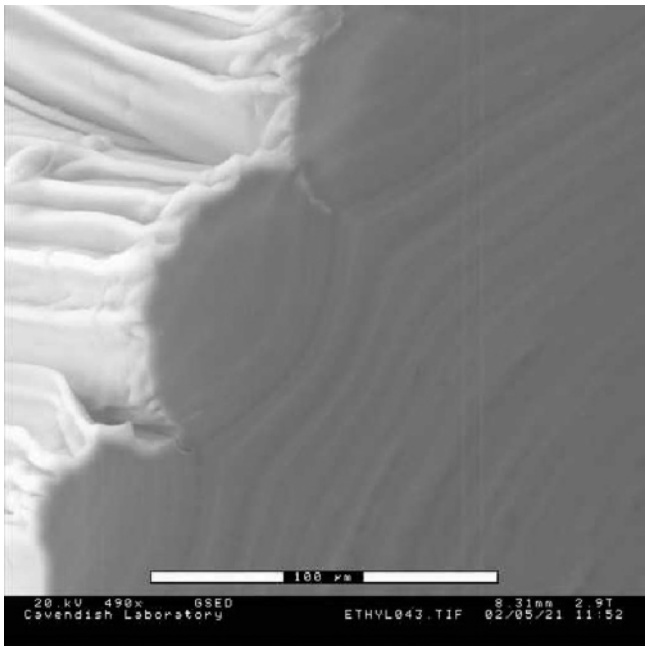

Figure 3. Image of the fractured edge of a sample, which shows wrinkles characterized by a primary and secondary length scale.

To understand the nature of the periodic bands that arise at moderate to large deformations, we look at a section of the sample (Figure 3) and see that the bands are a periodic modulation of the surface height; that is, they are wrinkles characterized by one or more typical length scales. This is similar to a number of different systems where wrinkles have been observed recently—thermal mismatch-induced wrinkles in metallic skin−polymer substrate systems,[11] and stretching-induced wrinkles in polydimethyl siloxane (PDMS) skin−PDMS substrate systems[12]—and suggests that we should be able to adapt a recent theory of wrinkling[13] to this situation. Dehydration of the sample, which typically occurs first on the surface, causes the formation of a skin on the gelatin gel that is typically much stiffer than the interior. In addition, the loss of water causes the skin to contract isotropically relative to the substrate, which is still hydrated. However, the presence of a substantial applied tension makes the stress on the skin highly anisotropic, causing the gel to contract laterally. When combined with the effect of the clamped boundaries, which prevent a uniform lateral contraction, this leads to a small compressive stress perpendicular to the direction of loading, causing the skin to buckle into a series of periodic wrinkles in a manner completely analogous to that of a stretched unsupported thin film.[13,14] The predictions of this theory have been verified qualitatively and quantitatively by recent experiments in a completely different system that bears some mechanistic resemblance to the drying gelatin: in PDMS rubbers subject to strain, exposure to ultraviolet/ozone radiation for extended periods of time causes the formation of skin with an enhanced stiffness over the first ∼5 nm of the sample. Wrinkles then appear when the strain is removed;[12] in fact, a hierarchical pattern of self−similar wrinkles appeared, just as predicted theoretically. A simple explanation for this secondary wrinkling in the drying gelatin is also the same as that for the PDMS system: once the primary short wavelength wrinkles are formed, further stretching causes the amplitude of these wrinkles to grow until saturation leads to an effective "skin" of wrinkles + substrate that is thicker than the original skin. This skin then wrinkles on even larger length scales (since it is stiffer) forming the type of pattern seen in Figure 3.

According to the theory of wrinkling,[13] the only required ingredients are a packing constraint, a skin that resists short wavelengths, and an underlying substrate that penalizes long wavelengths. The stretched gelatin film has all these ingredients; drying provides a skin on a soft substrate, while stretching the

(11) Bowden, N.; Brittain, S.; Evans, A. G.; Hutchinson, J. W.; Whitesides, G. W. *Nature* **1998**, *393*, 146−149.
(12) Efimenko, K.; Rackaitis, M.; Manias, E.; Vaziri, A.; Mahadevan, L.; Genzer, J. *Nat. Mater.* **2005**, *4*, 293−297.
(13) Cerda, E.; Mahadevan, L. *Phys. Rev. Lett.* **2003**, *90*, 74302.
(14) Cerda, E.; Ravi-Chandar, K.; Mahadevan, L. *Nature* **2002**, *419*, 579−580.

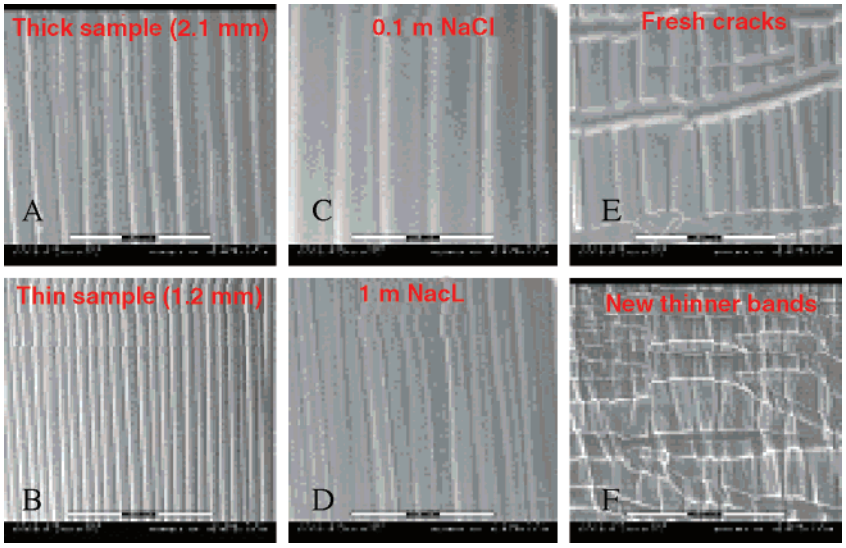

Figure 4. Variation of the wrinkling wavelength, with the sample thickness [(A) 2.1 mm and (B) 1.2 mm], with the amount of NaCl [(C) 0.1M and (D) 1M], and on the new thinner bands at the opening of the horizontal cracks (E,F).

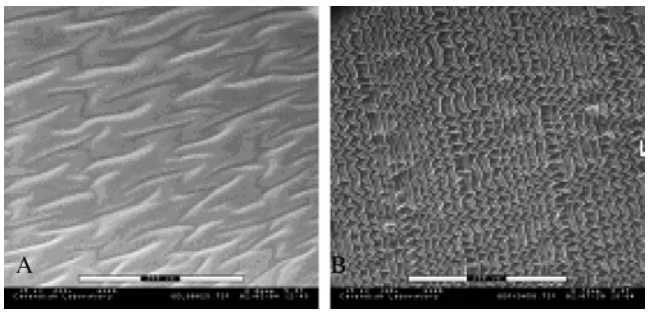

Figure 5. Bands relaxing after sample breakage, forming a different pattern.

film, combined with the inhomogeneous boundary conditions due to clamping, provides the contraction or packing constraint. For short wavelength wrinkles on a thick substrate, corresponding to the case here, the wavelength, λ, follows the scaling form[13]

$$\lambda \sim h\left(\frac{E_s}{E_b}\right)^{1/3} \tag{6}$$

where h is the thickness of the stiff skin, E_s is the modulus of this skin layer, and E_b is the modulus of the underlying bulk material. Before testing the theory quantitatively, we first check some of its simple qualitative predictions.

For the gelatin samples under study here, we believe that, despite our endeavors, limited water evaporation occurs at the sample surfaces, leading to the development of a stiffer surface layer relative to the bulk, fully hydrated gel. This is because, although conditions are set for the microscope to maintain the sample in an overall state of hydration, some dehydration of the sample at the surfaces is inevitable. Evidence for this skin is seen in Figure 3. Immersion of the whole sample in water rehydrates it to its original, homogeneous state with a uniform modulus throughout, and the bands disappear, as expected. Furthermore, covering the surface of the sample by cling film prior to straining suppresses the formation of the stripes. This observation lends weight to the idea that limited drying underlies band formation.

We also find that an increase in the gelatin concentration decreases the wavelength. This can be explained by the overall lower water content and, consequently, a reduced rate of evaporation leading to a lower contrast in the stiffness of the skin compared to that of the substrate E_s/E_b (and potentially also a thinner surface layer thickness h), and so λ is decreased. Increasing the salt concentration from 0.1 M NaCl (used for most experiments) to 1 M resulted in wrinkles with a shorter wavelength (Figure 4C,D) because increasing the salt content has the effect of lowering the water vapor pressure in the gel, thus reducing the rate of water loss. We observed that the wavelength decreases upon increasing the gelatin concentration as discussed above. An increase in strain rate provides less time for the water loss to proceed, which also promotes shorter wavelengths, again in line with the observation. Increasing the sample thickness also led to a larger wavelength (Figure 4A,B). This is because an increase in sample thickness reduces the effectiveness of the cooling of the sample from the stage that contacts the film only at its bottom. This will have the effect of increasing the rate of water loss for the top surface, increasing E_s and h, and thus the wrinkle wavelength.

Finally, fresh samples have smaller wavelengths than mature samples. Since we have seen that the origin of the surface skin lies in partial dehydration, the older a sample is, the more time there is for water loss, leading to a thicker and stiffer skin. Thus an older sample is predicted to have a larger wavelength, as is observed. Thus we can see that all our observations are consistent with the qualitative predictions based on eq 6, which interprets the bands as wrinkles induced by drying.

Testing eq 6 quantitatively requires information about the thickness and modulus of the skin, which are controlled by the kinetics of drying and thus change with time. Imaging the edge of the sample once it fails (Figure 3) allows us to estimate the thickness of the skin. To get an estimate of the modulus of the dehydrated skin and the hydrated bulk of the gelatin sample, we turn to the stress−strain curve (Figure 2) together with an image of the sample after failure. We approximate the modulus for the bulk of the sample from the early stages of deformation, from which we deduce $E_b \sim 35$ kPa. At late stages corresponding to large deformations, much of the gelatin film is dry, so that its response is a good approximation to that of the skin. This allows us to extract an approximate modulus of the skin, $E_s \sim 350$ kPa. We can also see from the image of the failure surface that a surface layer of about 5 μm (the "skin") appears appreciably different from the underlying material. Using this for the thickness of the skin in eq 6 yields $\lambda \sim 10$ μm, compared with the experimentally observed value of 9 μm. Given the crudity of the approximations made here, the agreement is excellent.

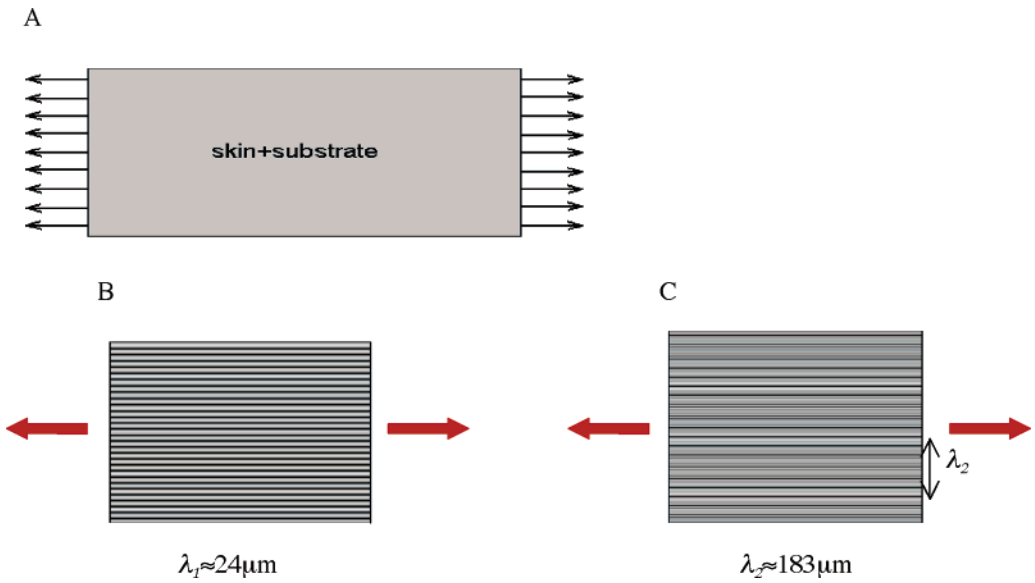

Figure 6. Results of a finite element simulation of the skin−substrate system under imposed uniaxial tensile strain. (A) Schematic of the skin + substrate systems under stretching. In the computations, a uniform stretching displacement is applied to the boundary of the skin−soft substrate system, while periodicity boundary conditions are imposed on the edges of the system. (B) By stretching the system, a periodic pattern of primary wrinkles with small wavelength appears on the skin. (C) As the stretching displacement proceeds, the amplitude of the first generation of wrinkles saturates, and a secondary wrinkling pattern on a much larger wavelength appears, thus forming the hierarchical nested buckling pattern. The contrast between the colors illustrates the out-of-plane displacement of the skin and its morphology; the modulation of the color represents the two wavelengths in the system.

To quantify this further and understand the reason for the hierarchical wrinkles, we carried out a computational study of the skin−substrate system using the same geometry as that used in the experiment, implemented in the commercial finite element package ABAQUS (Figure 6). The thin film (skin) is modeled as a linear elastic material, while the soft substrate of finite thickness is modeled as an incompressible hyperelastic material with a neo-Hookean model, which has a strain energy function $W = \mu/2\sum_{i=1}^{3}(\lambda_i^2 - 3)$, where λ_i are the principal stretches, which satisfy the relation $\lambda_1\lambda_2\lambda_3 = 1$ in light of incompressibility, and μ is the shear modulus of the material. The following parameter values were used: substrate shear modulus $\mu = 35$ kPa, skin thickness $h = 5\,\mu$m, skin shear modulus $G_B = 350$ kPa. The skin is assumed to be nearly incompressible. A uniform stretching displacement is applied to the boundary of the skin−soft substrate system, which leads to a periodic pattern of primary wrinkles of small wavelength, just as in a compressed film on a substrate.[12] As the strain increases, the amplitude of the first generation of wrinkles saturates. This leads to an effective skin of the gelatin that is a composite of the real skin and part of the substrate that is already buckled. Further stretching leads to the appearance of a secondary wrinkling pattern on much larger wavelength, which appears because of the buckling of an "effective skin" of much larger thickness, again, just as in the compressed film on a substrate studied recently.[12] The wavelength of the first generations is 24 μm, while that of the second generation is 183 μm. The discrepancy of the quantitative calculation with experiment is almost certainly due to the fact that the skin is not homogeneous through its thickness, so that its properties vary smoothly. This requires consideration of the material as one with graded properties rather than the simple discontinuity assumed here. Furthermore, the imposed boundary condition differs from the one employed in the experiment, which is only approximately consistent with a uniform stretching displacement imposed on the system. Thus, while the computations provide us with some insight into the underlying mechanism of the observed wrinkling and set the stage for a more thorough analysis of the various patterns that arise, more experiments are required to quantify the geometry of the skin and the kinetics of the process before we may proceed further.

4. Conclusions

The present work has shown the appearance of unexpected periodic structures under the large strain deformation of biopolymer gel systems, which form skins due to partial dehydration. We can understand these structures as wrinkles that form because of the differential strains that accompany the superficial drying of the gel that leads to the formation of a thin, dry, stiff skin which remains attached to the soft hydrated substrate. A number of qualitative predictions of this model are consistent with experiments to change the thickness of the skin, the elastic contrast between the skin and the substrate, and other sample and surface parameters. A simple computational model provides additional support for the proposed picture, but highlights the need for careful experiments to determine the input parameters such as the modulus of the drying skin and its thickness. This study has focused exclusively on the static equilibrium picture for the formation of these structures. An important next step is an understanding of the kinetics of drying of these hydrated polymeric materials that almost certainly go through a glassy phase associated with the formation of the stiff skin.

Acknowledgment. The authors thank the Product Microstructure Division of Unilever Research Colworth for their financial support of this research program, and for permission to publish this paper.

LA052343M